Refinery Downside Risk Hedging using Multivariate Price Modelling Including Transaction and Margin Costs

S. van der Heijden
Student no: 532033

July 28, 2021

Abstract

In this paper I minimise downside price risk for U.S. refineries using a model for the entire distribution of petroleum prices. I focus on out-of-sample hedging by modelling price changes with hierarchical outer power transformed Archimedian copulas (HOPACs). HOPACs may provide much needed stability, capture asymmetrical supply and demand characteristics of the underlying commodities and allow for non-normality. Furthermore, I include transaction and margin costs both in estimation and out-of-sample study, which are generally not included in literature. I find that HOPACs significantly improve hedging effectiveness relative to one-to-one hedging strategy for a value at risk objective, while minimising costs. I encourage managers to apply a HOPAC hedging strategy, which provides more downside risk protection for lower costs than the 'hard-to-beat' one-to-one hedging strategy.

Supervised by: dr. A.M. Camehl
Second assessor: J.A. Oorschot

ERASMUS UNIVERSITY ROTTERDAM
Erasmus School of Economics
Quantitative Finance

Contents

1 Introduction

Extreme volatility of crude and finished oil products prices during the COVID-19 pandemic shocked the oil refining industry as never before. The closing future price of crude oil with a delivery of one month reached a historic negative 38 $/barrel on 20 Apr 2020. During the pandemic, finished product prices, e.g. heating oil and gasoline, were reduced to one fourth of that years high, causing challenging risk management decisions for refineries. The product yield of a typical U.S. refinery can be approximated with the 3:2:1 crack spread, that measures the difference in purchasing price of three barrels of crude oil and selling price of two barrels of gasoline and one barrel of heating oil[1]. Historically, oil refineries have operated under relatively low margins. To hedge price risk in a low margin industry, oil refineries buy the crack spread, i.e. they buy crude oil futures and sell finished product futures (Energy Information Administration, 2002). The proportion of future contracts bought or sold relative to the spot contracts used for feedstock or produced as finished products are hedging ratios.

Adverse price movements, e.g. simultaneous increase in crude oil and decrease in finished product prices, are likely to push refineries in the red. For this purpose, Haigh and Holt (2002) estimate mean-variance multi-product crack-spread hedge ratios while accounting for time-varying covariability between energy prices. Moreover, Ji and Fan (2011) investigate a minimum-variance dynamic hedging approach for the crack-spread. Both studies assume normality in the disturbance terms. However, Lai (2012) shows that the joint distribution of spot and futures price changes are known to be skewed. Additionally, Lien and Tse (1998) show that corporate managers are less concerned by upside potential as they are with downside risk. Therefore, variance reduction may not be an adequate risk measure when returns are skewed. Furthermore, Alexander et al. (2013) finds that a one-to-one hedging strategy outperforms all variance reduction studies when incorporating transaction and margin costs. Moreover, they find that time series models perform poorly when costs are included, which may be caused by high transaction costs and instability in parameter estimates. Lui et al. (2017) are one of the few that investigate downside risk in crack-spread hedging using a kernel copula method on log re-

[1] See https://www.eia.gov/todayinenergy/includes/crackspread_explain.php for more information.

turns to examine minimum lower partial moment and variance as hedging objectives. However, uncommon news, e.g. the 1990 Iraqi invasion into Kuwait, can lead to jumps in prices (Chan & Maheu, 2002; Maheu & McCurdy, 2004). Consequently, log returns, can be a poor proxy for percentage returns. Sukcharoen and Leatham (2017) investigate several downside crack-spread risk measures on price returns by using Archimedean copulas and the more advanced vine copula models. They find that the symmetrical margins of Archimedean copulas are too restrictive, while vine copula models reduces risk for oil refineries significantly. However, model robustness is very important in hedging the crack spread, as fluctuating hedging-ratios can void the use of sophisticated price model building, since hedging costs can increase substantially relative to one-to-one hedging (Alexander et al., 2013). Furthermore, oil price volatility exhibits structural breaks and tends to increase altogether, favouring models that can accurately estimate on a shorter window (Peng et al., 2020; Salisu & Fasanya, 2013).

The aim of this research is to minimise downside risk of oil refineries using a multi-product hedging model. Multi-product refers to using several future contracts to hedge price risk exposure. This is in contrast to single-product hedging, which uses only one commodity to hedge price risk exposure. I use this approach for the different supply-demand dynamics of crude oil, heating oil and gasoline (The Energy Data Modeling Center, 2006). Moreover, I investigate optimal crack-spread hedging ratios on unfiltered[2] price changes in the refining industry with an out-of-sample hedging validation for several downside risk criteria, using a copula model. Furthermore, I model prices using a hierarchical multivariate price modelling approach, that allows for: (1) skewed price changes and asymmetric margins, (2) more intuitive and flexible dependence structures compared to simple Archimedean copulas, and (3) more parsimonious modelling than other sophisticated models (Ostap et al., 2013). A more parsimonious model can significantly reduce standard errors, relative to other sophisticated copulas, possible leading to more robust hedge-ratios and lower transaction and margin costs. Additionally, modelling price changes with a hierarchical model may be more logical, since spot and future price changes

[2]Some studies use filtered date to capture the time varying covariance structutes (e.g. Sukcharoen et al. (2015)). Other studies use unfiltered data (e.g. Sukcharoen and Leatham (2017)), to avoid errors in the estimation of conditional mean and variance models. Moreover, Alexander et al. (2013) shows GARCH models generate high transaction costs and instability in parameter estimates.

of commodities have related supply and demand dynamics (The Energy Data Modeling Center, 2006). Moreover, transaction and margin costs are included directly into the decision making process. This may improve the profitability of a historically low margin industry. To the best of my knowledge, this study is first in incorporating transaction and margin costs in the decision making process for downside risk hedging, using a model for the entire distribution of petroleum prices.

Given the skewed price changes and asymmetrical marginals of petroleum prices, modelling multi-product hedging ratios to minimise downside risk can be difficult. For this purpose, Sukcharoen and Leatham (2017) model the joint distribution of price changes with vine copulas. These copulas are very flexible and alleviate the aforementioned problems, but require many parameters to be estimated and do not seem to be supported by the logic in petroleum product markets. Consequently, the standard deviations of hedging ratios are relatively large, which may lead to higher transaction and margin costs. I deviate from Sukcharoen and Leatham (2017) by modelling price changes jointly with hierarchical outer power Archimedes copulas (HOPACs) and test the performance against industry-standard fully-hedged one-to-one hedging strategy (Alexander et al., 2013). HOPACs allow for the more technical properties of Sukcharoen and Leatham (2017) models, e.g. asymmetry and non-normality, while staying true to the supply and demand characteristics of petroleum product markets, e.g. structure dependence between difference products. Górecki et al. (2021) introduce a construction and estimation technique for HOPACs that allow for a good fit in the body and tail, skewness, asymmetry, and robust estimation. Additionally, I introduce an estimation technique by incorporating transaction and margin costs from Alexander et al. (2013) directly into the hedge-ratio estimation for downside risk measures, which voids the use sophisticated models in a variance reduction setting (Alexander et al., 2013).

To hedge the crack spread, I consider weekly spot and future price data from 17 Mar 1995 to 12 Mar 2021. The spot and future prices are West Texas Intermediate (WTI) crude oil at Crushing Oklahoma, regular unleaded gasoline at New York Harbour (NYH), RBOB regular gasoline at NYH, and no. 2 heating oil at NYH. Furthermore, I use 3-month Treasury Bill yields and ICE BofA BBB U.S. corporate index yields from 17 Mar 2000 to 22 Jan 2021 to compute margin costs for the hedging strategy. The 3-month Treasury Bill yields are used as a proxy for the interest received on a future margin account, while the BBB U.S. corporate index yields are used as a proxy for the cost of capital for a typical U.S. refinery to initiate the margin (Alexander et al., 2013).

I compare value at risk and expected shortfall hedging effectiveness (HE) at a weekly frequency of a HOPAC hedging strategy to a one-to-one hedging strategy and find that HOPAC hedging usually outperforms one-to-one hedging in an out-of-sample setting when trading excluded from estimation. Furthermore, including transaction and margin costs in estimation successfully increases profitability, while always outperforming one-to-one hedging. In sum, managers that are interested in downside risk hedging of oil refineries should consider modelling price changes with HOPACs to provide more downside risk protection for lower costs relative to the 'hard-to-beat' one-to-one hedging strategy.

2 Data

2.1 Spot and Future Prices

I obtain spot prices per barrel for crude oil, gasoline and no. 2 heating oil, from 17 Mar 1995 to 22 Jan 2021 at a weekly frequency (3 times 1349 observations) from the U.S. Energy Information Administration[3]. These are West Texas Intermediate (WTI) crude oil at Crushing Oklahoma, regular unleaded gasoline at New York Harbour (NYH), and no. 2 heating oil at NYH. Furthermore, I obtain one and two months to delivery future prices per barrel, for crude oil, gasoline and no. 2 heating oil, from 17 Mar 1995 to 12 Mar 2021, at a weekly frequency (3 times 1349 observations), from the U.S. Energy Information Administration. These are WTI crude oil at Crushing Oklahoma, regular unleaded gasoline at NYH, RBOB regular gasoline at NYH, and no. 2 heating oil at NYH. I construct gasoline future data by concatenating regular unleaded gasoline (17 Mar 1995 to 29 Dec 2006) and RBOB regular gasoline (5 Jan 2007 to 12 Mar 2021), as unleaded gasoline futures were faced out. RBOB regular gasoline spot prices are unavailable to me, so I use regular unleaded gasoline spot prices for the entire window, as

[3]See https://www.eia.gov/petroleum/data.php for more information.

supply and demand trends are the same for both types of gasoline (Alexander et al., 2013). As such, they are highly correlated[4].

First, I transform the data by converting gasoline and no. 2 heating oil to dollar per barrel. Second, price changes are computed by taking the first discrete difference over time for all series. Third, I convert the futures to a continuous series. This can be done with the constant-maturity or roll-over method. Alexander et al. (2013) shows that the roll-over method creates artificial jump caused by seasonality of heating oil and gasoline. These jumps produce outliers that are detrimental to tail risk analysis and are not present in continuous series constructed with constant-maturity method. By using Galai's (1979) constant-maturity return-index method, I can construct continuous futures that provide realisable investments, which is crucial for my hedging analysis. I follow the adaptation of the method by Alexander et al. (2013), which is given by,

$$\Delta F_{t,T} = \eta_t \Delta F_{t,T_1} + (1 - \eta_t) \Delta F_{t,T_2}, \quad 0 \leq \eta_t \leq 1 \tag{1}$$

where $\Delta F_{t,T_1}$ and $\Delta F_{t,T_2}$ are constant maturity futures expiring in T_1 and T_2, respectively, and η_t is given by,

$$\eta_t = \frac{T_2 - (t + T)}{T_2 - T_1}, \quad T_1 < T < T_2 \tag{2}$$

where T is equal to 44 calendar days, which is always between the first and second contract time to expiry (Alexander et al., 2013). Fourth, similarly to Alexander et al. (2013) and Sukcharoen and Leatham (2017), I remove the price data during extreme market conditions of Hurricane Katrina from 29 Aug 2005 to 9 Sep 2005, where I assume no trades are taking place, which is realistic as most production was shut down. Finally, the 3:2:1 crack spread is computed, by subtracting 2 barrels of gasoline and 1 barrel of heating oil, from 3 barrels of crude oil.

Table 1 shows that mean and median for weekly price changes are small in comparison to the standard deviation. Additionally, the standard deviations for finished products are higher than the standard deviation of the crude oil. Moreover, the difference between the minimum and maximum is smallest for no. 2 heating oil, followed by crude oil, and largest for gasoline. Taken together, these findings indicate that symmetrical marginals in the model may be too

[4] $\rho_{\text{spearman's}} = 0.97$ for weekly Los Angeles RBOB and NYH unleaded gasoline from 12 Sep 2003 to 12 Mar 2021.

Table 1: Summary statistics for weekly crude oil spot price change (ΔS^C), gasoline spot price change (ΔS^G), heating oil spot price change (ΔS^H), crude oil futures price change (ΔF^C), gasoline future price change (ΔF^G), heating oil future price (ΔF^H) change from 24 Mar 1995 to 12 Mar 2021 (6 times 1357 observations). JB refers to the Jarque-Bera test statistic, where * shows rejection of null hypothesis of normality at 1% significance. Furthermore, ADF refers to the Augmented Dickey-Fuller (with intercept and trend) test statistic, where * shows rejection of null hypothesis that price changes follow a unit root process at 1% significance. Finally, LB refers to the Ljung–Box test statistic, where where * shows rejection of null hypothesis that price changes are independently distributed at 1% significance.

	ΔS^C	ΔS^G	ΔS^H	ΔF^C	ΔF^G	ΔF^H
Mean	0.026	0.034	0.033	0.026	0.031	0.035
Median	0.130	0.168	0.084	0.120	0.197	0.082
S.D.	2.361	2.968	2.652	2.235	2.794	2.497
Skewness	-0.557	-0.555	-0.289	-0.634	-0.746	-0.306
Kurtosis	6.540	3.072	3.211	5.189	3.814	2.818
Min	-16.800	-18.816	-14.196	-14.445	-19.272	-14.392
Max	13.930	12.516	12.810	11.649	10.837	10.276
JB	2452.363*	594.012*	592.335*	1589.655*	934.556*	462.762*
ADF	-10.120*	-11.717*	-10.497*	-9.982*	-9.982*	-10.152*
LB	58.874*	80.511*	90.944*	74.119*	82.010*	87.856*

restrictive. Skewness and excess kurtosis show signs of non-normality for both the feedstock and finished products. I reject the null of the Jarque-Bera test, and therefore I should take non-normality into account. Moreover, the augmented Dickey-Fuller (ADF), with trend and intercept, is rejected, hence a stationary model is suitable. Additionally, I reject the Ljung-Box test, so the series may not be independently distributed, which should be taken into account. Table 2 shows all correlations are positive and correlation is highest between price changes of the spot/future pairs for each commodity, with crude oil being highest, followed by heating oil, while being lowest for gasoline. Therefore, a structured model that links spot/future pairs is fitting.

Table 2: Kendall's tau for weekly crude oil spot price change (ΔS^C), gasoline spot price change (ΔS^G), heating oil spot price change (ΔS^H), crude oil futures price change (ΔF^C), gasoline future price change (ΔF^G), heating oil future price (ΔF^H) change from 24 Mar 1995 to 12 Mar 2021 (6 times 1356 observations).

	ΔS^C	ΔS^G	ΔS^H	ΔF^C	ΔF^G	ΔF^H
ΔS^C	1.000	0.521	0.618	0.898	0.574	0.646
ΔS^G		1.000	0.528	0.532	0.732	0.546
ΔS^H			1.000	0.629	0.573	0.857
ΔF^C				1.000	0.587	0.660
ΔF^G					1.000	0.597
ΔF^H						1.000

Figure 1 shows considerable changing co-movement between spot and future prices for crude oil, gasoline and heating oil. Furthermore, non-constancy of the variance of price changes can be observed. Both can be explained by evolving supply and demand characteristics, as this is the most important fundamental factor in petroleum product markets. For example, before the 'Shale Revolution' from 2010-2012, when large reserves of WTI light sweet crude oil[5] was rediscovered in the U.S. most finished products were refined from heavy and sour middle eastern oil. Higher supply of WTI post Shale Revolution may have caused the divergence of WTI and finished products, while U.S. refineries still use heavy sour middle eastern oils as feedstock because the plants are not fitted for higher quality oils. Additionally, control over prices substantially decreased when the free-market U.S. production industry gained market share, which was a different dynamic compared to the grip of the Organization of the Petroleum Exporting Countries (OPEC) prior to the Shale Revolution.

Prices are relatively stable until 2004, when strong economic growth boosts world oil demand. Oil prices peaked in 2008 when demand was at an all time high and spare production capacity in OPEC countries was diminished, prior to collapsing as the world heads into the Great Recession.

[5] called 'sweet' for the low sulfur content and 'light' for the lower density, which is easier to crack into finished products

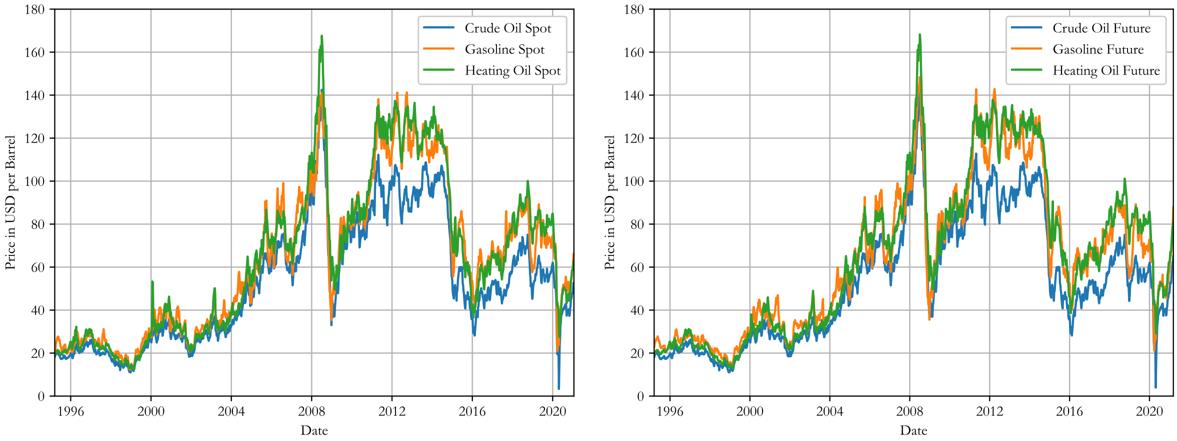

(a) (b)

Figure 1: (a) Spot prices of crude oil, gasoline and heating oil from 14 Mar 1995 to 12 Mar 2021, at a weekly frequency (6 times 1357 observations), (b) contract 1 future prices of crude oil, gasoline and heating oil from 14 Mar 1995 to 12 Mar 2021, at a weekly frequency (6 times 1357 observations)

Prices recovered, until declining sharply in 2014, as US shale oil production growth increases supply, while demand stayed relatively flat. Not long after, prices crash in 2020 when demand evaporates, as the world goes into lockdown due to the COVID-19 pandemic, with daily crude oil futures prices going negative on 20 Apr 2020. Figure 2a shows that the 3:2:1 crack spread appears to be very volatile from 17 Mar 1995 to 12 Mar 2021. Furthermore, prices come close to zero often, indicating low margins for refineries are common.

2.2 Interest Rates

I obtain 3-month Treasury Bill yields (r_f) and ICE BofA BBB U.S. corporate index yields (r_d) from 17 Mar 2000 to 22 Jan 2021, at a weekly frequency (2×1087 observations), from the St. Louis Federal Reserve Economic Database[6]. Figure 2b shows higher volatility for r_d relative to r_f. Furthermore, Federal Reserve fund rate adjustments are clearly visible in r_f, when fund rates are lowered following the 2000, 2008 and 2020 recessions, and raised from 2004 and 2016 onward. Moreover, large spikes are visible in r_d, especially at the start of the 2008 and 2020

[6]See https://fred.stlouisfed.org/ from more information.

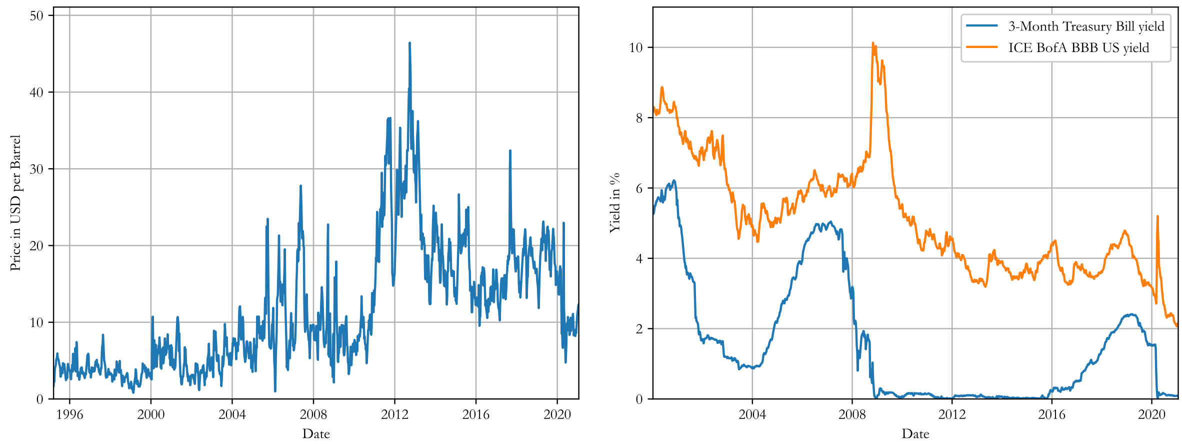

(a) (b)

Figure 2: (a) 3:2:1 crack spread from 14 Mar 1995 to 12 Mar 2021, at a weekly frequency (6×1357 observations), (b) 3-month Treasury Bill yields and ICE BofA BBB U.S. corporate index yields from 17 Mar 2000 to 22 Jan 2021, at a weekly frequency (2×1087 observations).

recession. Furthermore, the difference between r_d and r_f can increase substantially, when the federal reserve lowers rates to stimulate the economy, while investors demand higher yields on corporate debt.

3 Hedging the Crack Spread

3.1 Profit and Loss

The profit margin at a typical U.S. refinery can be replicated by selling a 3:2:1 crack spread. That is, buying three barrels of crude oil and selling two barrels of gasoline and one barrel of heating oil. Managers at refineries are in two markets: feedstock which they buy, and finished products which they sell. The difference between the feedstock and finished products determines the gross profit, and thus is of great importance. In reality, a single refinery cannot be approximated by the 3:2:1 crack spread, as it outputs a vast range of different products, from light gasses such as methane, to heavy speciality products such as bitumen. However, on average, the 3:2:1 crack spread is a good approximation for the gross profit of a refining company, averaged over a portfolio of refining plants[7] (Alexander et al., 2013; Sukcharoen & Leatham, 2017).

Low profit margins are typically hedged by buying crack spread futures, i.e. selling crude oil futures and buying gasoline and heating oil futures (Energy Information Administration, 2002). Following Haigh and Holt (2002), I assume that a refinery buys the crack spread at period $t-1$ and sells the position at period t, where the periods are weekly. Consequently, the refineries hedged profit per barrel $\pi(\boldsymbol{b})$ is given by,

$$\pi_t(\boldsymbol{b}_{t-n}) = -S_t^{\mathrm{C}} + \frac{2}{3}S_t^{\mathrm{G}} + \frac{1}{3}S_t^{\mathrm{H}} + b_{t-n}^{\mathrm{C}}(F_t^{\mathrm{C}} - F_{t-1}^{\mathrm{C}}) - \frac{2}{3}b_{t-n}^{\mathrm{G}}(F_t^{\mathrm{G}} - F_{t-1}^{\mathrm{G}}) - \frac{1}{3}b_{t-n}^{\mathrm{H}}(F_t^{\mathrm{H}} - F_{t-1}^{\mathrm{H}}), \quad (3)$$

where C, G, H denote crude oil, gasoline and heating oil, respectively, S_t^i for $i \in \{\mathrm{C}, \mathrm{G}, \mathrm{H}\}$ refer to the spot prices, F_t^i for $i \in \{\mathrm{C}, \mathrm{G}, \mathrm{H}\}$ denote the future prices, and $\boldsymbol{b}_{t-n} = (b_{t-n}^{\mathrm{C}}, b_{t-n}^{\mathrm{G}}, b_{t-n}^{\mathrm{H}})'$ are hedging ratios determined at $t-n$ for $n \in \mathbb{N}$. All prices at period t are random variables, whereas prices at period $t-n$ are known. Furthermore, I assume all spot and future transactions occur simultaneously.

The hedged profit per barrel in (3) can be rewritten into price changes by adding and subtracting the spot price for crude oil, two-thirds heating oil and one-thirds gasoline. Following, Alexander et al. (2013), the hedged portfolio profit and losses $\Delta\pi_t(\boldsymbol{b}_t)$ is obtained by disregarding one negative crude oil, and two-thirds positive gasoline and one-thirds positive heating oil spot price at $t-1$, given by,

$$\begin{aligned} \Delta\pi_t(\boldsymbol{b}_{t-n}) &= -\Delta S_t^{\mathrm{C}} + \frac{2}{3}\Delta S_t^{\mathrm{G}} + \frac{1}{3}\Delta S_t^{\mathrm{H}} + b_{t-n}^{\mathrm{C}}\Delta F_t^{\mathrm{C}} - \frac{2}{3}b_{t-n}^{\mathrm{G}}\Delta F_t^{\mathrm{G}} - \frac{1}{3}b_{t-n}^{\mathrm{H}}\Delta F_t^{\mathrm{H}}, \\ &= \mathbf{1}_3{}' \cdot \Delta\boldsymbol{S}_t + \boldsymbol{b}_{t-n}' \cdot \Delta\boldsymbol{F}_t \end{aligned} \quad (4)$$

where, $\Delta\boldsymbol{S}_t = (-\Delta S_t^{\mathrm{C}}, \frac{2}{3}\Delta S_t^{\mathrm{G}}, \frac{1}{3}\Delta S_t^{\mathrm{H}})'$, $\Delta\boldsymbol{F}_t = (\Delta F_t^{\mathrm{C}}, -\frac{2}{3}\Delta F_t^{\mathrm{G}}, -\frac{1}{3}\Delta F_t^{\mathrm{H}})'$, $\mathbf{1}_3$ is a [3x1] matrix of ones, and $\Delta\pi_t(\boldsymbol{b}_{t-n}) = \pi_t(\boldsymbol{b}_{t-n}) + (S_{t-1}^{\mathrm{C}} - \frac{2}{3}S_{t-1}^{\mathrm{G}} - \frac{1}{3}S_{t-1}^{\mathrm{H}})$.

3.2 Transaction and Margin Costs

In this section I follow Alexander et al. (2013) in incorporating margin and transaction costs, that may be crucial for hedging effectiveness. A representative refinery will incur transaction

[7] See tinyurl.com/3vjmbc3k and tinyurl.com/3rhs93xs for more information.

costs from from the bid-ask spread and the round tip commission charged by the exchange. The bid-ask spread is defined as the difference between the bid and ask price, divided by the middle price. Refineries cannot buy or sell the middle price. Consequently, a seller will only receive as much as the bid, which is lower than the middle price, and a buyer will have to pay the ask, which is higher than the middle price. This leads to neglecting costs when only the middle price is used. A refinery will also incur margin cost that arise from the initial margin and paying interest on the maintenance margin. Initial margin is the required amount a refinery must deposit into its account to enter the future contract. Interest costs arise from the cost of debt of the maintenance margin. I assume the refinery will only place market orders, disregarding any possible hedging unrelated trading gains, only taking liquidity from the market.

Commission costs for a one-to-one hedge of the crack spread, i.e. all hedge ratios are equal to one, at the New York Mercantile Exchange is \$1.45 per $1,000$ barrel contract. To illustrate, assume a refinery wishes to fully hedge $300,000$ barrels of crude oil to sell as finished products. Using a 3:2:1 crack spread, this would result in purchasing 300 crude oil future contracts, and selling 200 gasoline and 100 heating oil future contracts. The commission associated with this trade would be $300 \cdot \$1.45 = \$435$. The commission cost for re-balancing λ_t^{com} is given by,

$$\lambda_t^{\text{com}}(\Delta \boldsymbol{b}_{t-n}) = \frac{3|b_{t-n}^{\text{C}} - b_{t-n-1}^{\text{C}}| + 2|b_{t-n}^{\text{G}} - b_{t-n-1}^{\text{G}}| + |b_{t-n}^{\text{H}} - b_{t-n-1}^{\text{H}}|}{6} \cdot P \tag{5}$$

where P is the commission per crack spread ($\$1.45/1000 = \$0.00145$), and the fraction is an approximation for the number of 3:2:1 crack spread bundles.

The dollar value of the bid-ask spread $\lambda_t^{\text{bid-ask}}$ is given by,

$$\lambda_t^{\text{bid-ask}}(\Delta \boldsymbol{b}_{t-n}) = F_t^{\text{C}}|b_{t-n}^{\text{C}} - b_{t-n-1}^{\text{C}}|\delta^{\text{C}} + \frac{2}{3}F_t^{\text{G}}|b_{t-n}^{\text{G}} - b_{t-n-1}^{\text{G}}|\delta^{\text{G}} + \frac{1}{3}F_t^{\text{H}}|b_{t-n}^{\text{H}} - b_{t-n-1}^{\text{H}}|\delta^{\text{H}}, \tag{6}$$

where δ^i for $i \in \{\text{C}, \text{G}, \text{H}\}$ is the bid-ask spread for each commodity. Following Dunis et al. (2008), I set δ^i to 1 bps, 10 bps, 12 bps for crude oil, gasoline and heating oil, respectively.

The initial margin for a refinery that sells the crack spread expiring in one month, at the New York Mercantile Exchange, is \$11 for a 3:2:1 crack spread bundle. The total cost for raising the initial margin is given by,

$$m_t^{\text{initial}}(\boldsymbol{b}_{t-n}) = \frac{3|b_{t-n}^{\text{C}}| + 2|b_{t-n}^{\text{G}}| + |b_{t-n}^{\text{H}}|}{6} N(r_t^d - r_t^f) \tag{7}$$

where, N is the initial margin per crack spread, r_t^d is the cost of raising the initial margin and r_t^f is the risk free rate returned from depositing in the margin account. Modelling interest rates is out of the scope of this study. As such I assume both r_t^d and r_t^f are known at $t-1$. Furthermore, the refinery will raise debt in order to finance the initial margin. The top three U.S. refineries, i.e. Marathon Petroleum, Valero Energy and Phillips 66, are rated BBB by S&P Global Ratings. Therefore, I use a BBB corporate yield index as a proxy for r_t^d. For r_t^f, I use the 3-month Treasury Bill yield.

As I use weekly data, the daily changes in the margin account, or mark-to-market, are linearly approximated. The weekly interest on the margin account is given by,

$$m_t^{\text{m2m}}(\boldsymbol{b}_{t-n}) = \frac{1}{2}(-3b_{t-1}^{\text{C}}\Delta F_t^{\text{C}} + 2b_{t-1}^{\text{G}}\Delta F_t^{\text{G}} + b_{t-1}^{\text{H}}\Delta F_t^{\text{H}})r_t^f. \tag{8}$$

which is negligible when interest rates go to zero. The total optimal hedged portfolio profit and losses $\Delta\pi_t^*(\boldsymbol{b^*}_t)$ are given by,

$$\Delta\pi_t^*(\boldsymbol{b}_{t-n}) = \Delta\pi_t(\boldsymbol{b}_{t-n}) + m_t^{\text{m2m}}(\boldsymbol{b}_{t-n}) - m_t^{\text{initial}}(\boldsymbol{b}_{t-n}) - \lambda_t^{\text{bid}-\text{ask}}(\Delta\boldsymbol{b}_{t-n}) - \lambda_t^{\text{commission}}(\Delta\boldsymbol{b}_{t-n}) \tag{9}$$

where $\boldsymbol{b}_{t-n}$ contains the updated optimal hedging ratios.

To the best of my knowledge, this study is first to include the transaction and margin costs directly into the optimisation process. As such, the objective of the refinery is to minimise downside risk of $\Delta\pi_t^*(\boldsymbol{b}_{t-n})$ by selecting the optimal $\boldsymbol{b}_{t-n}^*$, or

$$\boldsymbol{b}_{t-n}^* = \arg\min_{\boldsymbol{b}_{t-n}} Risk(\Delta\pi_t^*(\boldsymbol{b}_{t-n})) \tag{10}$$

where $Risk(\Delta\pi_t^*(\boldsymbol{b}_{t-n}))$ is defined as the downside risk of $\Delta\pi_t^*(\boldsymbol{b}_{t-n})$.

3.3 Downside Risk Measures

I consider two downside risk measures[8]. First, the widely used value at risk (VaR), is the quantile of the loss distribution G, defined by,

$$\text{VaR}_\alpha = \inf\{l \in \mathbb{R} : G_L(l) \geq \alpha\}, \tag{11}$$

[8] I note that the literature uses other risk measures also, such as lower partial moment and semi-variance. These are excluded for practical reasons as they would not change the result.

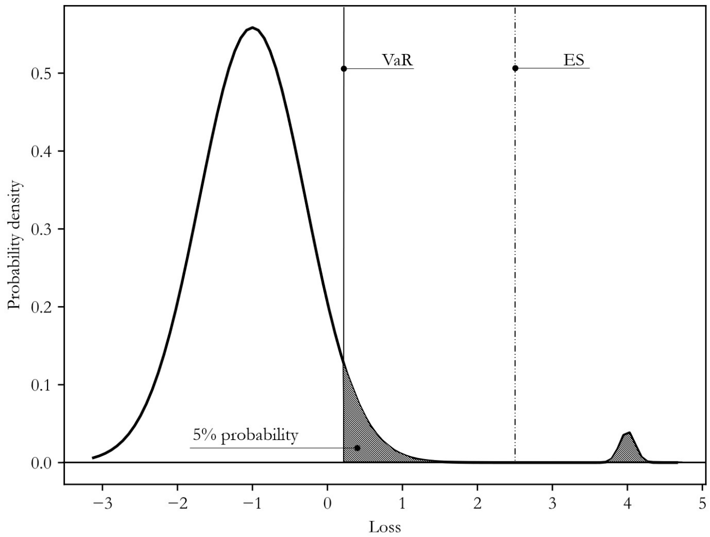

Figure 3: Example of losses represented by normal mixture distribution with 95% VaR and ES denoted by horizontal line and horizontal dotted line, respectively.

where, $\alpha \in (0, 1)$ is a confidence level (McNeil et al., 2015). Second, I use expected shortfall (ES), which is closely related to the VaR, defined by,

$$\text{ES}_\alpha = \frac{1}{1-\alpha} \int_\alpha^1 q_u(G_L) du, \tag{12}$$

where $q_u(G_L) = G_L^{\leftarrow}(u)$ is the quantile function of G_L (McNeil et al., 2015). For both VaR_α and ES_α, I set $\alpha \in \{0.9, 0.93, 0.95, 0.98, 0.99\}$.

Figure 3 gives an example of the VaR and ES under losses of a normal mixture distribution. VaR is the loss that occurs with a probability of α, which is 5% in this case. When the data is discontinuous it is represented by closest value below the probability α. This gives insight into a single value on the loss distribution. One disadvantage of VaR is that it does not give any insight into the distribution of losses above the $1 - \alpha$ threshold. This is not relevant when losses are normally distributed, since the probability distribution is monotonically decreasing in the upper tail. However, when this is not the case, such as in Figure 3, VaR gives poor insight into the expectation of losses. This is where ES enters the field, by estimating the expectation of losses above the $1 - \alpha$ threshold. The two statistics can differ substantially when very large losses due to supply and demand shocks are probable.

I follow McNeil et al. (2015) in estimating the VaR and ES by first ranking the losses $L_1, \dots, L_n$ as $L_{(1)} \leq L_{(2)} \leq \cdots \leq L_{(n)}$, for $n \in \mathbb{N}$. Then, the estimator of VaR is given by,

$$\hat{\text{VaR}} = L_{(\lceil n\alpha \rceil)}. \tag{13}$$

Furthermore, the estimator of the ES is given by,

$$\hat{\text{ES}} = \frac{\lceil n\alpha \rceil - n\alpha}{n(1-\alpha)} L_{(\lceil n\alpha \rceil)} + \frac{1}{n(1-\alpha)} \sum_{i=\lceil n\alpha \rceil + 1}^{n} L_{(i)}. \tag{14}$$

4 Price Model

4.1 Multivariate Copula

I use a multivariate copula approach to model the joint distribution of changes in spot and future prices, $\Delta \boldsymbol{S}_t$ and $\Delta \boldsymbol{F}_t$, respectively. This is required to solve (10), since $\Delta \boldsymbol{S}_t$ and $\Delta \boldsymbol{F}_t$ are the only unknowns and the calculation of downside risk measures depends on the entire distribution.

A copula is a distribution function that links marginal distributions to a joint distribution (copula is 'link' in Latin). Copulas allow for a bottom-up model-building approach, which is useful in risk management, since marginal behaviour of risk factors is generally better understood than their dependence structure (McNeil et al., 2015). Additionally, copulas can allow for skewness and asymmetrical marginals. Furthermore, they allow for relatively easy sampling, which is particularly useful in determining downside risk measures using Monte Carlo simulation (McNeil et al., 2015). Copula models are based on Sklar (1957) theorem, which states that any joint distribution function F, with marginals $F_1, \dots, F_d$ for $d \in \mathbb{N}$, can be linked together with a copula $C : [0,1]^d \to [0,1]$. Mathematically this is given by,

$$F(x_1, \dots, x_d) = C(F_1(x_1), \dots, F_d(x_d)), \tag{15}$$

where $x_2, \dots, x_d \in \mathbb{R}$.

Archimedean copulas (AC) have proven particularly useful in risk management applications, for allowing asymmetry in the joint tails, i.e. upper tail may be different from lower tail dependence. The $d-$dimensional case for $d \geq 2$ of this particular copula family is given by,

$$C_\psi(u_1, \ldots, u_d;\ \theta) = \psi_\theta(\psi_\theta^{-1}(u_1) + \cdots + \psi_\theta^{-1}(u_d)). \tag{16}$$

where $u_1, \ldots, u_d \in [0, 1]$ are uniform random variables, $\theta \in \mathbb{R}$, the generator $\psi(\cdot) : [0, \infty) \to [0, 1]$ is a continuous and decreasing function that satisfies $\psi(0) = 1$ and $\lim_{t\to\infty} \psi(t) = 0$ and is imposed to be completely monotonic to guarantee a proper copula (McNeil et al., 2015).

ACs have several limitations. First, most ACs are one parametric, that generally relates the parameter to the Kendall's tau dependence measure. This allows for efficient sampling techniques and likelihood inference. However, the model may fit well in the body, while the fit in the tail is poor. This is particularly relevant in likelihood inference, where the fit in body and tail is treated equally, while tail observations occur less often. Second, symmetry in ACs can be restrictive when modelling in large dimensions. This implies that the dependence between all pairs of components is equal. It seems plausible that different supply and demand dynamics between different commodities result in asymmetries. Finally, the unstructured nature of ACs can be limiting when structure is present in the data, e.g. when supply and demand dynamics are similar between spot and future pairs of the same commodity.

Górecki et al. (2021) proposes to alleviate these limitations by combining outer power ACs (OPACs) and hierarchical ACs (HACs). First, outer power transformations add an additional parameter to the generator, that allows for a good fit in body and tail. Second, HACs are constructed by nesting several ACs within one another, allowing for a asymmetrical model, and adding much needed structure (Joe, 1997).

Nelsen (2006) proposes that an outer power transformation of any generator of a 2-d AC generator creates a generator again and is given by,

$$\psi_{\beta,\theta}(t) = \psi_\theta(t^{\frac{1}{\beta}}) \tag{17}$$

where $\beta \in [1, \infty)$. The additional parameter β allows for fine-tuning the fit in the tail while fixing the models Kendall's tau, thus keeping a good fit in the body.

HACs can be constructed by replacing some arguments of ACs with other (H)ACs (Joe,

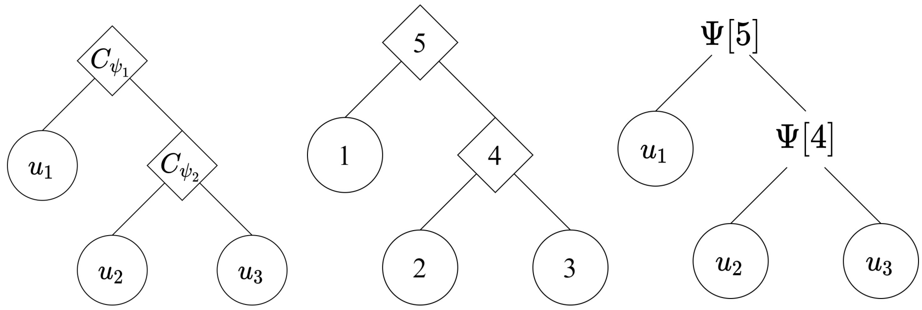

(a) (b) (c)

Figure 4: (a) A tree-like representation of (18), (b) An undirected tree with with nodes $\nu = \{1, 2, \ldots, 5\}$ and $\varepsilon \subset \nu \times \nu$, and (c) A tree-like representation with fork mapping from (20) (Górecki et al., 2021).

1997). For a 3-variate HAC, this is given by,

$$C_{\psi_1,\psi_2}(u_1, u_2, u_3;\ \theta_1, \theta_2) = C_{\psi_1}\{u_1, C_{\psi_2}(u_2, u_3;\ \theta_2);\ \theta_1\}. \tag{18}$$

where, C_{ψ_1} and C_{ψ_2} are both Archimedean copulas. It should be noted that decomposition in (18) is not unique and the dimension is chosen for illustrative purposes only, which I will use throughout the methodology. Figure 4a shows a tree-like representation of (18).

Following Górecki et al. (2021), (18) can be described using graph theory. An 'undirected tree' with nodes $\nu = \{1, 2, \ldots, m\}$ for $m = 2d-1$ and $\varepsilon \subset \nu\times\nu$ can be derived by enumerating its nodes. For example, Figure 4b shows that $\nu = \{1, 2, \cdots, 5\}$ and $\varepsilon = \{(1, 5),\ (2, 4),\ (3, 4),\ (4, 5)\}$. Nodes $\{1,\ 2,\ 3\}$ correspond to the 'leaves' of the tree, while $\{4,\ 5\}$ are 'forks'. Leaves are given by the variables u_1, u_2 and u_3 in the HAC structure. The forks correspond to C_{ψ_1} and C_{ψ_2}, which are set uniquely according to the ranking of dependence measure Kendall's tau (τ), such that node m has the lowest τ, followed by node $m-1$, etc. The highest fork is referred to as the 'root'.

Rewriting (18) using a labelling function Ψ, that maps the fork to the generators gives,

$$C_{\Psi[5],\Psi[4]}(u_1, u_2, u_3) = C_{\Psi[5]}\{u_1, C_{\Psi[4]}(u_2, u_3)\}, \tag{19}$$

where $\Psi[4]$ maps fork node 4 to ψ_{θ_2} and $\Psi[5]$ maps fork node 5 to ψ_{θ_1}. Equation 19 allows me to express $C_{\psi_1,\psi_2}(u_1, u_2, u_3)$ in terms of (ν, ε, Ψ) which is useful in estimation and sampling. The arguments of $C_{\Psi[4]}$ in Equation 19, i.e. 2 and 3, correspond to the 'children' of fork 4, and the arguments of $C_{\Psi[5]}$, i.e. 1 and 4, correspond to the 'children' of fork 5. This structure allows the HAC, with arbitrary dimension, to be written as $C(\nu, \varepsilon, \Psi)$. Figure 4c shows a graphical representation of Equation 19.

Finally, the aforementioned OPAC and HAC example are combined to from a 3-variate HOPAC, which is given by,

$$C(\nu, \varepsilon, \Psi) = C_{\Psi[5]}\{u_1, C_{\Psi[4]}(u_2, u_3)\}, \tag{20}$$

where $\nu = \{1, 2, \cdots, 5\}$, $\varepsilon = \{(1,5),\ (2,4),\ (3,4),\ (4,5)\}$, $\Psi[4] = \psi(\theta_2, \beta_2)$, and $\Psi[5] = \psi(\theta_1, \beta_1)$.

Equation 20 can be extended to a d-variate model as long as the 'sufficient nesting conditions' are satisfied, which they are when the first derivative of $\Psi[i]^{-1} \circ \Psi[j]$, where i is the parent of j, is continuously monotone for all parent-child pairs (McNeil, 2008). Sufficient nesting conditions are satisfied for HOPACs (Górecki et al., 2021).

4.2 Estimation

I follow Górecki et al. (2021) in estimating HOPACs. Three steps are necessary in estimating HOPACs, (1) determining structure, i.e. the general form of the tree, (2) deciding on the AC family used, and (3) the estimating parameters for each fork.

Górecki et al. (2017) proposes an estimation approach to determine the structure of an HAC, which is independent of the AC family. Consequently, this approach can directly be implemented to estimate the structure of an HOPAC. All that is required to estimate the structure are the pairwise Kendall's taus.

The structure is estimated as follows. First, I estimate all pair-wise sample Kendall's taus τ_{ij}, for $i, j \in \{1, \ldots, m\}$, $m \in \mathbb{N}$, and set $\hat{\nu} := \{1, \ldots, 2m-1\}, \hat{\varepsilon} := \emptyset$ and $\mathcal{I} := \{1, \ldots, m\}$, where m is the number of leaves. Second, I find the two nodes in $\mathcal{I}$ to join,

$$(i, j) = \underset{\tilde{i}<\tilde{j},\ \tilde{i}\in\mathcal{I},\ \tilde{j}\in\mathcal{I}}{\operatorname{argmax}} \operatorname{avg}((\tau_{\tilde{\tilde{i}}\tilde{\tilde{j}}})_{(\tilde{\tilde{i}},\tilde{\tilde{j}})\in\downarrow(\tilde{i})\times\downarrow(\tilde{j})}) \tag{21}$$

where, $\downarrow(\tilde{i}) \in \{1, \ldots, m\}$ are the descendant leaves of fork $i \in \{m+1, \ldots, 2m-1\}$. Third, I update $\hat{\varepsilon} := \hat{\varepsilon} \cup \{(i, m+k), (j, m+k)\}$. Fourth, I remove i and j from $\mathcal{I}$ and add $m+k$, i.e.

Table 3: Four popular families of completely monotone outer power transformed generators with the range of the original parameter θ, generator function, and upper-lower tail dependence coefficients. Lower tail dependence λ_l is given by $\lim_{q \downarrow 0} C(q,q)/q$ and upper tail dependence λ_l is given by $2 - \lim_{q \downarrow 0} \{1 - C(1-q, 1-q)\}/q$ (McNeil et al., 2015). Furthermore, $\beta \in [1, \infty)$ is the outer power transform parameter.

Generator (a)	Range θ_a	$\psi_{a,\theta,\beta}(t)$	λ_l	λ_u
Ali-Mikhai-Haq (A)	$[0, 1)$	$\frac{1-\theta}{\exp(t^{1/\beta})-\theta}$	0	$2-2^{1/\beta}$
Clayton (C)	$(0, \infty)$	$(1+\theta t^{1/\beta})^{-1/\theta}$	$2^{-1/\theta\beta}$	$2-2^{1/\beta}$
Frank (F)	$(0, \infty)$	$\frac{-\log\{1-(1-\exp(\theta))\exp(-t^{1/\beta})\}}{\theta}$	0	$2-2^{1/\theta\beta}$
Joe (J)	$[1, \infty]$	$1-(1-\exp(-t^{1/\beta}))^{1/\theta}$	0	$2-2^{1/\theta\beta}$

$\mathcal{I} := \mathcal{I} \cup \{m+k\} \setminus \{i, j\}$. Finally, I repeat steps one trough five for $k = \{2, \ldots, m-1\}$ to obtain the structure of $C(\nu, \varepsilon, \Psi)$ as $C(\hat{\nu}, \hat{\varepsilon}, \Psi)$.

As an example, I walk through estimating the simple structure of (18). Starting at $k = 1$, $\hat{\nu} := \{1, \ldots, 5\}, \hat{\varepsilon} := \emptyset$ and $\mathcal{I} := \{1, \ldots, 3\}$. I estimate τ_{ij} for $i, j \in \{1, 2, 3\}$, which results in a 3×3 matrix. Next, I find (i, j) in (21). Let me assume this is the $i = 3$, $j = 2$ pair, since $\text{avg}(\tau_{32}, \tau_{23})$ is the maximum. Second, I update $\hat{\varepsilon} := \{(2, 4), (3, 4)\}$ and $\mathcal{I} := \{1, 4\}$. Moreover, I set $k = 2$, and find $(i, j) = (4, 1)$, since $\text{avg}(\tau_{21}, \tau_{31}, \tau_{12}, \tau_{13})$ is the maximum. Furthermore, I update $\hat{\varepsilon} := \{(1, 5), (2, 4), (3, 4), (4, 5)\}$ and $\mathcal{I} := \{5\}$. Now that the structure is estimated, I can continue estimating $\hat{\Psi}$. For this, I need to select HOPAC generators first.

I consider four popular completely monotone generator families. These are, Ali-Mikhai-Haq (A), Clayton (C), Frank (F) and Joe (J), shown in Table 3. The well known Gumbel generator is excluded, since the outer power transformed generator is equal to the original generator.

To estimate the parameters of the HOPAC structure, I turn to Górecki et al. (2021) top-down estimator. The estimator requires $\hat{\nu}$, $\hat{\varepsilon}$, and a generator family a as input, and returns the parameter estimates of all forks $\hat{\Psi}[k] \leftarrow \psi_{(a,\hat{\theta},\hat{\beta})}$ for $k \in \{m+1, \ldots, 2m-1\}$. Following Górecki et al. (2021), to obtain a proper copula from completely monotone generators, I use the restrictions:

- if $\beta_{parent} = 1$, then $\theta_{child} \geq \theta_{parent}$ and $\beta_{child} \geq \beta_{parent}$, or

- if $\beta_{parent} > 1$ then $\theta_{child} = \theta_{parent}$ and $\beta_{child} \geq \beta_{parent}$.

Intuitively, these restrictions enforce that the dependence increases when moving from the root to the leaves of the three.

To estimate the parameters, I traverse the structure, i.e. starting at the root fork of the copula, going through all of the forks. First, I find the children (i, j) of the root. Second, the descendant leaves of the children are stored, i.e. $l_i \leftarrow$ descendent leaves of i, if i is a fork, else $l_i \leftarrow \{i\}$. The same is done for j. Third, I preform maximum likelihood estimation (MLE) over all combinations of l_i and l_j and take the average,

$$(\hat{\theta}, \hat{\beta}) \leftarrow \frac{1}{\#(l_i) \cdot \#(l_j)} \sum_{\tilde{i} \in l_i} \sum_{\tilde{j} \in l_j} \underset{(\theta_{\tilde{i}\tilde{j}}, \beta_{\tilde{i}\tilde{j}}) \in \theta_a \times [1, \infty)}{\operatorname{argmax}} \sum_{m=1}^{n} \log c_{\psi_{a, \theta_{\tilde{i}\tilde{j}}, \beta_{\tilde{i}\tilde{j}}}} (u_{m\tilde{i}}, u_{m\tilde{j}}) \tag{22}$$

where $\#$ is the number of element, c is the density of the copula, θ_a is the parameter range from Table 3, and u_{mi} for $m \in \{1, \ldots, n\}, i \in \{1, \ldots, d\}$ are the pseudo-observations of the sample, e.g. $d = 3$ and $n = 1000$ from Figure 4. Fourth, I set $\Psi[2d - 1] \leftarrow \psi_{a, \hat{\theta}, \hat{\beta}}$. Fifth, check which of the two restrictions apply, and use it with steps one through five on the children of the current fork, until all parameters are estimated. I use maximum likelihood estimation since it is unbiased, naturally extends to any parameter dimension, and statistically more efficient than Kendall's tau inverse and distance-based estimator (Górecki et al., 2021).

As an example, I walk through estimating the parameters of the simple structure of (18). Starting at the root, i.e. $k = 5$, I find the children of this fork to be $(1, 4)$. Next, $l_i = \{1\}$ and $l_j = \{2, 3\}$. Moreover, I perform MLE 2×1 times and take the average to obtain $\Psi[5] \leftarrow \psi_{a, \hat{\theta}, \hat{\beta}}$. Furthermore, I use $(\hat{\theta}, \hat{\beta})$ to set restrictions on the parameters of $\Psi[4]$. Finally, I preform MLE once, since $\Psi[4]$ only has children that are leaves, using the aforementioned restrictions. With $\Psi[4] \leftarrow \psi_{a, \hat{\theta}, \hat{\beta}}$, I have estimated the entire distribution in (18).

4.3 Simulation

In this section I zoom in on the simulation that is required to compute optimal hedge ratios for downside risk objectives. Below I present McNeil (2008) simulation method for hierarchical copulas, under the assumption that $\psi_1, \ldots, \psi_d$ are Laplace-Stieltjes (LS) transformed Archimedean

Table 4: Explicit inverse Laplace-Stieltjes transforms of Archimedean copula generators (Hofert, 2010). Geo refers to the geometric distribution and Γ refers to the gamma distribution.

Generator(a)	G_1
Ali-Mikhai-Haq(A)	$\mathrm{Geo}(1-\theta)$
Clayton(C)	$\Gamma(1/\theta, 1)$
Frank(F)	$\log\left(1-e^{-\theta}\right)$
Joe(J)	$\binom{1/\theta}{k}(-1)^{k-1}, k \in \mathbb{N}$

copula generators. Solving (10) requires the entire distribution of hedged portfolio profits and losses, that I obtain by means of Monte Carlo simulation. Sampling is based on representing (16) as a mixture distribution with LS transforms, first derived by Joe (1997).

The mixture presentation of a d-variate HAC is given by,

$$\begin{aligned} &C_d\left(u_1,\ldots,u_{d+1};\psi_1,\ldots,\psi_d\right) \\ &\quad= \int_0^\infty P_1^{v_1}\left(u_1\right) C_{d-1}\left(P_1^{v_1}\left(u_2\right),\ldots,P_1^{v_1}\left(u_{d+1}\right);\psi_2^{(1)}\left(\cdot;v_1\right),\ldots,\psi_d^{(1)}\left(\cdot;v_1\right)\right)\mathrm{d}G_1\left(v_1\right) \\ &\quad= \int_0^\infty\cdots\int_0^\infty P_1^{v_1}\left(u_1\right)\cdots P_d^{v_d}\left(u_d\right)P_d^{v_d}\left(u_{d+1}\right)\mathrm{d}G_d\left(v_d;v_{d-1}\right)\cdots\mathrm{d}G_2\left(v_2;v_1\right)\mathrm{d}G_1\left(v_1\right) \end{aligned} \tag{23}$$

where G_1 is the distribution function with LS transform ψ_1, $P_k(u) = \exp(-\psi_k^{-1}(u))$ for $k \in \{1,\ldots,d\}$ and $G_k(v;v_{k-1})$ is the distribution function with LS transformations $\psi_k^{(k-1)}(\cdot;v_{k-1}) = \exp\left(-v_{k-1}\psi_{k-1}^{-1}\circ\psi_k(\cdot)\right)$ for $k \in \{2,\cdots,d\}$.

I follow the steps from McNeil (2008) to sample from (23). First, I generate variate V_1 with distribution function G_1 from Table 4. Second, I follow Hofert (2011) to include the outer power transform in sampling. I let ψ_β for $\beta \in [1,\infty)$ be the outer power transformation of a continuously monotone generator. Then, $\dot{V} = SV^\beta$, where $V \sim G$, $S \sim \mathrm{St}(1/\beta, 1, \cos^\beta(\pi/2\beta), \mathbf{1}_{\beta=1}; 1)$, where St is the stable distribution. Third, I generate variates V_k for $k \in \{2,\ldots,d\}$ with distribution function $G_k(v;V_{k-1})$, where $k-1$ is the index of the parent of k, and is given by,

$$G_k(v;V_{k-1}) = \exp\left(-V_{k-1}\left[\psi_{k-1}^{-1}\left\{\psi_{k-1}\left(t^{\frac{1}{\beta_2}}\right)\right\}\right]^{\beta_1}\right) = \exp\left(-V_{k-1}t^{\frac{\beta_1}{\beta_2}}\right), \tag{24}$$

where the right-hand-side is the Gumbel generator provided that $\beta_1 \leq \beta_2$, which is enforced by the restrictions. I follow Hofert (2011) to sample Equation 24 with Laplace-Stieltjes transform given by,

$$\mathrm{St}\left(\beta_1/\beta_2, 1, \left\{\cos\left(\frac{\beta_1}{\beta_2}\frac{\pi}{2}\right)V_{k-1}\right\}^{\frac{\beta_2}{\beta_1}}, V_{k-1}\mathbf{1}_{\{\beta_1/\beta_2=1\}}; 1\right). \tag{25}$$

Third, I generate independent uniform variate $(X_1, \ldots, X_{d+1})$. Finally, I return $(U_1, \ldots, U_{d+1})$ where $U_i = \psi_i\left(-\ln\left(X_i\right)/V_i\right)$ for $i \in \{1, \ldots, d\}$ and $U_{d+1} = \psi_d\left(-\ln\left(X_{d+1}\right)/V_d\right)$. These are converted back to price changes using empirical distribution of price changes of the respective window.

Following Sukcharoen and Leatham (2017), I estimate the HOPAC structure and parameters in a five year (261 weeks) moving window approach on the pseudo-observations of the six commodity price changes, for each generator in Table 3. Pseudo-observations are constructed by determining the rank of each price change in the window and dividing by the window length plus one. It should be noted that some studies estimate the model using GARCH filtered data, e.g. Sukcharoen et al. (2015). However, similar to Sukcharoen and Leatham (2017) I deviate from this method to avoid first-stage estimation errors, which have been shown to cause parameter instability, and subsequently may void the use of HOPACs by causing under-performance when costs are included (Alexander et al., 2013). The moving windows result in 4×1095 model estimates, one for each HOPAC generator. Next, I simulate $4 \times 6 \times 10,000$ (4 generators, 6 price change series) draws from each model and compute the optimal hedging ratio $\boldsymbol{b}^*$ with the Nelder and Mead (1965) direct search method in (10). Following Alexander et al. (2013), I compute the portfolio profit and losses for (1) a fully hedged one-to-one strategy, i.e. all hedge-ratios are equal to one, and (2) the optimal hedge-ratios under the HOPAC model.

Finally, I compare the hedging effectiveness and gross margin. Hedging effectiveness (HE) is a measure to determine whether the model performs better or worse relative to a one-to-one hedging strategy. Furthermore, mean gross margin (GM) is important for managers as it determines the profitability of refineries. The hedging effectiveness is given by,

$$\mathrm{HE}_j = \left(1 - \frac{Risk_\alpha(\Delta\pi_t^*(\boldsymbol{b}_t^*))}{Risk_\alpha(\Delta\pi_t^*(\mathbf{0}))}\right) \tag{26}$$

where $j \in \{N, A,\ C,\ F,\ J\}$ (Table 3), $\pi_t^*(\mathbf{0})$ is the unhedged P/L, and $Risk_\alpha$ refers to either

VaR or ES at confidence level $1-\alpha$ (Sukcharoen & Leatham, 2017). Furthermore, when $j = N$ then b_t^* is equal to a $[3 \times 1]$ matrix of ones to replicate one-to-one hedging.

The mean gross margin of the one-to-one hedging strategy is given by,

$$\mathrm{GM_N} = \frac{1}{n}\sum_{i=1}^{n} \frac{\pi_i(\mathbf{1}_3)}{S_i^C} \tag{27}$$

where, $\mathbf{1}_3$ is a $[3 \times 1]$ matrix of ones, n is the total number of windows. Additionally, the mean gross margin under the HOPAC model is given by,

$$\mathrm{GM_k} = \frac{1}{n}\sum_{i=1}^{n} \frac{\pi_{ij}(\boldsymbol{b}_{i-1})}{S_i^C}. \tag{28}$$

where $k \in \{A,\ C,\ F,\ J\}$. Finally, I compare gross margins of one-to-one versus HOPAC models with,

$$\Delta\mathrm{M_k} = \mathrm{GM_k} - \mathrm{GM_N}. \tag{29}$$

A similar formula is used when including transaction and margin costs.

Table 5: The three different scenarios ordered by their estimation and out-of-sample method.

Out-of-sample \ Estimation	No costs	Costs
No costs	Scenario 1	-
Costs	Scenario 2	Scenario 3

To evaluate the performance of the modelling approach I consider different scenarios. Table 5 shows these scenarios. The first scenario is achieved by excluding costs in the estimation process and out-of-sample study. The second scenario is given by excluding costs in estimation, but including costs out-of-sample, and is used to compare the result to Alexander et al. (2013). The third scenario is achieved by including costs in both the estimation and out-of-sample study.

5 Results

This section compares effectiveness of the HOPAC hedging strategy to a one-to-one hedging strategy in an out-of-sample context. Several steps are required to achieve this goal. First, I estimate the hierarchical structure of the model over a moving window from 17 Mar 2000 to 15 Jan 2021 with a window size of 261 weeks. Second, I estimate the model parameters over the aforementioned windows with generator functions given in Table 3 and compare the model fit. Third, I simulate price changes and estimate hedging ratios with and without inclusion of costs in estimation. Fourth, optimal forecast lag is discussed to circumvent first stage estimation errors introduced by filtering. Finally, I compare hedging effectiveness of the HOPAC strategy under different generators to one-to-one heding in an out-of-sample context. Additionally, profitability is compared between including and excluding costs in estimation and I zoom in on transaction and margin costs, to give insight on the importance of different costs.

5.1 Structure

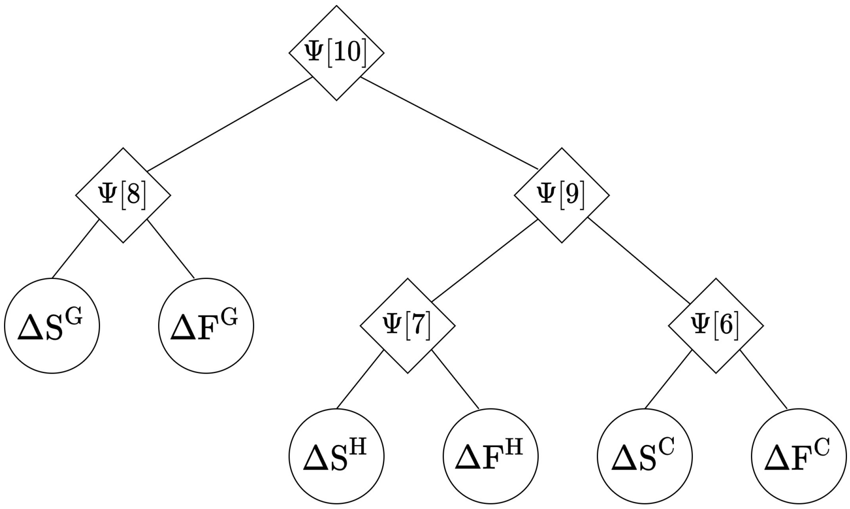

Figure 5: Estimated structure from 17 Mar 2000 with a window size of 261 weeks.

Figure 5 shows the estimated structure on unfiltered price changes for 17 Mar 2000, with a window size of 261 weeks (estimated on 24 Mar 1995 to 17 Mar 2000), which is equal for all four generators. The estimated structures from 24 Mar 2000 to 15 Jan 2021 are mostly identical to that of 17 Mar 2000, except for an uncommon switch between $\Psi[8]$ and $\Psi[9]$. Unsurprisingly, the spot and future pair for each commodity are linked together. Furthermore, crude oil is linked in the first fork ($\Psi[6]$), followed by heating oil in the second fork ($\Psi[7]$). These are nested in the fourth fork ($\Psi[9]$), indicating higher dependence of crude oil and heating oil, than crude oil/heating oil and gasoline. Gasoline is linked in the third fork ($\Psi[8]$), which is nested with $\Psi[9]$ in the root ($\Psi[10]$). When $\Psi[8]$ and $\Psi[9]$ are switched, cross-dependence between crude oil and heating oil is slightly higher than the gasoline pair. Taken together, the stability of the estimated structures confirms the choice for a hierarchical model.

The structure in Figure 5 can be explained by supply and demand characteristics of crude oil, heating oil and gasoline. Historically, consumers increase demand of heating oil during cold weather and winter storms, which generally coincides with higher crude oil prices as winter storms interrupt delivery systems[9]. Furthermore, demand for gasoline increases during spring and late summer, when consumer drive more, causing higher prices. Additionally, refineries are required due to regulation to replace cheaper but more evaporative gasoline with more expensive less evaporative gasoline in summer [10]. These characteristics cause lower dependence for crude with gasoline than heating oil, thus explaining the body of the structure in Figure 5.

5.2 Model Fit

In this section I provide evidence of the benefit of HOPACs using Akaike information criterion (AIC). Figure 6 shows the AIC for the Ali-Mikhai-Haq, Clayton, Frank, and Joe generated HOPACs averaged over the nodes ($\frac{1}{5}\sum_{i=6}^{10} \mathrm{AIC}_{\Psi[i]}$) with estimated structure from Mar 17 2000 to 15 Jan 2021 (1087 AIC averages per model). The Ali-Mikai-Haq, Clayton and Frank HOPAC models perform relatively well. Furthermore, the Frank HOPAC shows the lowest AIC average, followed by Ali-Mikai-Haq, Clayton and Joe HOPAC. Interestingly, the Joe model shows a relatively poor fit, although the difference is small. Additionally, all HOPAC models show a better fit than a Clayton HAC model, which confirms the choice for the outer-power transform.

[9]see https://www.eia.gov/energyexplained/heating-oil/factors-affecting-heating-oil-prices.php for more information.

[10]see https://www.eia.gov/energyexplained/gasoline/price-fluctuations.php for more information.

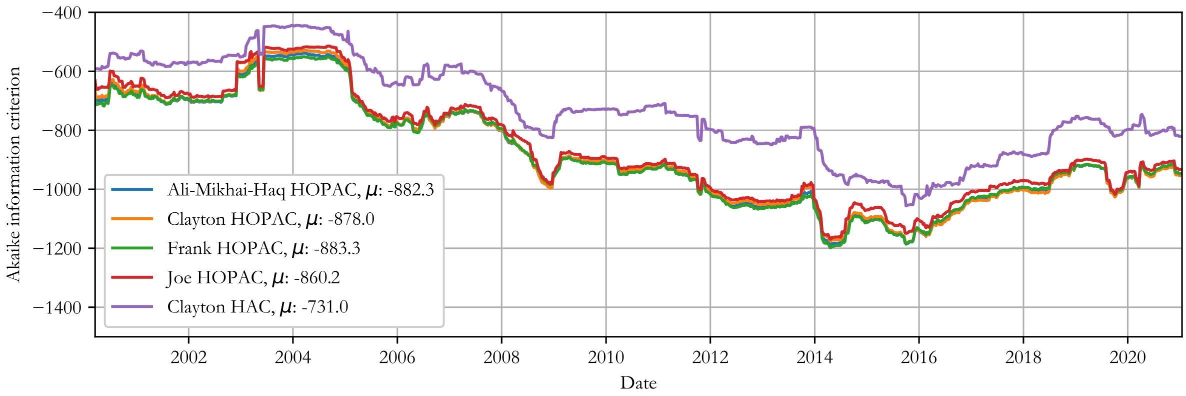

Figure 6: Ali-Mikhai-Haq, Clayton, Frank and Joe HOPAC, and Clayton HAC Log-likelihood averaged over nodes from Mar 17 2000 to Jan 15 2021 (1087 observations).

5.3 Hedging Ratios Estimates

In preparation for the out-of-sample study I estimate optimal hedging ratios for the different generators under two downside risk measures. Table 6 and Table 7 shows VaR and ES, mean hedge ratio estimates and standard deviations, for $1 - \alpha = \{0.9, 0.93, 0.95, 0.98, 0.99\}$, from 17 Mar 2000 to 15 Jan 2020 with and without costs in estimation, respectively. On average, hedge ratios are between 0.75 and 1.12 when costs are excluded in estimation and between 0.60 and 1.09 when costs are included in estimation. Furthermore, mean hedge ratios appear to be higher for heating oil, while hedge ratios of gasoline are lower when costs are excluded than crude oil. This may be explained by the higher dependence between the long position in heating oil and short position in crude oil compared to the long position in gasoline and short position in crude oil, for positive hedging ratios. Interestingly, Sukcharoen and Leatham (2017) did not find a meaningfull difference in hedging ratios between heating oil and gasoline using vine copulas and Alexander et al. (2013) found much higher hedging ratios for OLS and autocorrelation based models. Hedge ratios appear to be relatively flat for different confidence levels when cost are excluded, while increasing over confidence levels when costs are included on average. Thus, when costs are included in estimation, the model proposes a more 'risk-off' hedging strategy when managers are concerned for higher confidence levels. It seem logical that this can be explained by costs being more relevant at lower confidence level, while becoming less relevant as the confidence level increases. Surprisingly, hedge ratios are mostly lower for ES than VaR ceteris paribus, while ES is a higher tail risk measure than VaR for equal confidence level.

Standard deviations appear to increase substantially when costs are included in estimation, possibly due to higher variability due to interest costs. Furthermore, standard deviations decrease over higher VaR confidence level when costs are included. It seems plausible that introducing costs in estimation adds noise, e.g. interest rate volatility, that becomes less important when the confidence level increases and big losses become more relevant. Furthermore, ES takes the entire tail into account in estimation and is consequently less effected by this effect. Standard deviation are substantially lower than the vine copula based hedging ratios by Sukcharoen and Leatham (2017) and OLS and auto-correlation based hedging ratios by Alexander et al. (2013). Alexander et al. (2013) shows that instability in parameter estimates cause unusually high hedging ratios which may also be the culprit in Sukcharoen and Leatham (2017) method.

Table 6: Mean optimal hedge ratios with standard deviation in parentheses for different generators (a) and risk measures excluding costs in estimation from 17 Mar 2000 to 15 Jan 2021. Var and ES refer to value at risk and expected shortfall, respectively. Generators are Ali-Mikai-Haq (A), Clauton (C), Frank (F) and Joe (J).

a	Risk Measure									
	VaR					ES				
	90%	93%	95%	98%	99%	90%	93%	95%	98%	99%
Panel A: Crude oil hedge ratios										
A	0.92(0.06)	0.93(0.06)	0.94(0.06)	0.96(0.06)	0.96(0.09)	0.86(0.07)	0.86(0.08)	0.86(0.10)	0.84(0.14)	0.84(0.15)
C	0.92(0.06)	0.93(0.06)	0.93(0.06)	0.95(0.07)	0.95(0.08)	0.85(0.06)	0.85(0.07)	0.84(0.09)	0.82(0.13)	0.82(0.13)
F	0.92(0.06)	0.93(0.06)	0.94(0.06)	0.96(0.07)	0.95(0.10)	0.86(0.07)	0.86(0.08)	0.86(0.10)	0.85(0.14)	0.84(0.15)
J	0.93(0.06)	0.94(0.06)	0.95(0.06)	0.97(0.07)	0.97(0.09)	0.86(0.07)	0.86(0.08)	0.85(0.10)	0.84(0.15)	0.83(0.17)
Panel B: Heating Oil hedge ratios										
A	1.12(0.11)	1.11(0.10)	1.10(0.10)	1.09(0.10)	1.09(0.11)	1.01(0.13)	1.01(0.14)	1.01(0.15)	1.02(0.19)	1.03(0.23)
C	1.12(0.10)	1.11(0.10)	1.11(0.10)	1.10(0.10)	1.09(0.10)	1.00(0.12)	1.00(0.13)	1.00(0.14)	1.01(0.20)	1.02(0.27)
F	1.12(0.10)	1.11(0.10)	1.10(0.10)	1.10(0.11)	1.10(0.11)	1.03(0.13)	1.03(0.14)	1.03(0.15)	1.05(0.20)	1.06(0.26)
J	1.12(0.11)	1.12(0.11)	1.12(0.11)	1.11(0.11)	1.10(0.11)	0.98(0.12)	0.97(0.12)	0.97(0.13)	0.97(0.16)	0.97(0.19)
Panel C: Gasoline hedge ratios										
A	0.86(0.11)	0.87(0.11)	0.87(0.12)	0.89(0.12)	0.89(0.13)	0.83(0.10)	0.83(0.10)	0.83(0.11)	0.82(0.12)	0.81(0.13)
C	0.86(0.11)	0.87(0.11)	0.87(0.12)	0.88(0.12)	0.90(0.13)	0.83(0.1)	0.83(0.10)	0.83(0.11)	0.82(0.12)	0.81(0.14)
F	0.85(0.11)	0.86(0.11)	0.87(0.11)	0.88(0.11)	0.89(0.13)	0.82(0.10)	0.82(0.10)	0.82(0.11)	0.81(0.12)	0.81(0.13)
J	0.84(0.12)	0.83(0.12)	0.83(0.12)	0.83(0.13)	0.83(0.14)	0.78(0.10)	0.78(0.10)	0.77(0.11)	0.76(0.12)	0.75(0.14)

Table 7: Mean optimal hedge ratios with standard deviation in parentheses for different generators (a) and risk measures including costs in estimation from 17 Mar 2000 to 15 Jan 2021. VaR and ES refer to value at risk and expected shortfall, respectively. Generators are Ali-Mikai-Haq (A), Clauton (C), Frank (F) and Joe (J).

a	Risk Measure									
	VaR					ES				
	90%	93%	95%	98%	99%	90%	93%	95%	98%	99%
Panel A: Crude oil hedge ratios										
A	0.62(0.36)	0.70(0.26)	0.75(0.22)	0.85(0.16)	0.89(0.15)	0.64(0.22)	0.66(0.21)	0.67(0.21)	0.69(0.22)	0.70(0.21)
C	0.62(0.36)	0.70(0.26)	0.74(0.23)	0.83(0.17)	0.87(0.17)	0.62(0.22)	0.64(0.21)	0.65(0.21)	0.66(0.22)	0.68(0.20)
F	0.63(0.33)	0.69(0.26)	0.74(0.22)	0.86(0.16)	0.89(0.16)	0.64(0.21)	0.67(0.20)	0.68(0.20)	0.71(0.21)	0.72(0.20)
J	0.64(0.31)	0.72(0.24)	0.76(0.21)	0.87(0.16)	0.90(0.15)	0.66(0.20)	0.68(0.19)	0.69(0.20)	0.70(0.22)	0.71(0.22)
Panel B: Heating Oil hedge ratios										
A	0.72(0.65)	0.84(0.49)	0.91(0.41)	1.04(0.25)	1.08(0.18)	0.61(0.32)	0.64(0.29)	0.66(0.27)	0.72(0.25)	0.77(0.25)
C	0.75(0.67)	0.84(0.49)	0.89(0.45)	1.04(0.25)	1.06(0.20)	0.60(0.32)	0.62(0.29)	0.64(0.27)	0.69(0.25)	0.74(0.26)
F	0.77(0.62)	0.85(0.49)	0.92(0.41)	1.04(0.23)	1.09(0.17)	0.64(0.31)	0.68(0.29)	0.7(0.27)	0.77(0.25)	0.82(0.27)
J	0.75(0.60)	0.85(0.48)	0.91(0.43)	1.05(0.27)	1.09(0.18)	0.61(0.32)	0.64(0.29)	0.66(0.27)	0.71(0.24)	0.73(0.24)
Panel C: Gasoline hedge ratios										
A	0.69(0.16)	0.73(0.13)	0.75(0.13)	0.81(0.13)	0.84(0.14)	0.76(0.11)	0.77(0.11)	0.78(0.11)	0.77(0.11)	0.76(0.12)
C	0.69(0.16)	0.73(0.13)	0.75(0.12)	0.8(0.13)	0.83(0.14)	0.75(0.10)	0.76(0.10)	0.77(0.11)	0.77(0.12)	0.76(0.13)
F	0.67(0.16)	0.71(0.14)	0.74(0.13)	0.81(0.13)	0.83(0.15)	0.75(0.11)	0.76(0.10)	0.77(0.11)	0.77(0.11)	0.77(0.12)
J	0.67(0.15)	0.7(0.13)	0.71(0.12)	0.75(0.12)	0.77(0.14)	0.71(0.10)	0.72(0.10)	0.72(0.10)	0.72(0.11)	0.72(0.13)

5.4 Optimal Forecast Window

In this section I apply a heuristic approach to circumvent the first stage estimation errors introduced by filtering. As noted before, auto-correlation may be present in price changes and should be taken into account. I tackle this issue by introducing a time lag between estimating hedging ratios and the trading date. Figure 7 shows the number of positive differences between HOPAC and one-to-one hedging strategy HE to total number of HEs under HOPAC hedging strategy for scenario two and three (2 scenarios $\times$ 4 HOPACs $\times$ 10 risk measures $= 2 \times 40$ HEs), for lags ranging from 1 to 261 weeks. Furthermore, HEs are computed with the entire loss distribution from from 24 Mar 2000 to 22 Jan 2021 (1087 observations per distribution). The fraction generally increases over the forecast window n up to roughly 20 weeks, after which it stays flat in scenario two and decreases for scenario three. It seems plausible that autocorrelation causes the i.i.d. assumption only to be valid when hedging ratios are estimated up to roughly 20 weeks in advance. Additionally, when the estimation is more than 20 weeks prior to trading, information in the data becomes decreasingly additive to hedging, especially in scenario 3, where cost information is used in estimation.

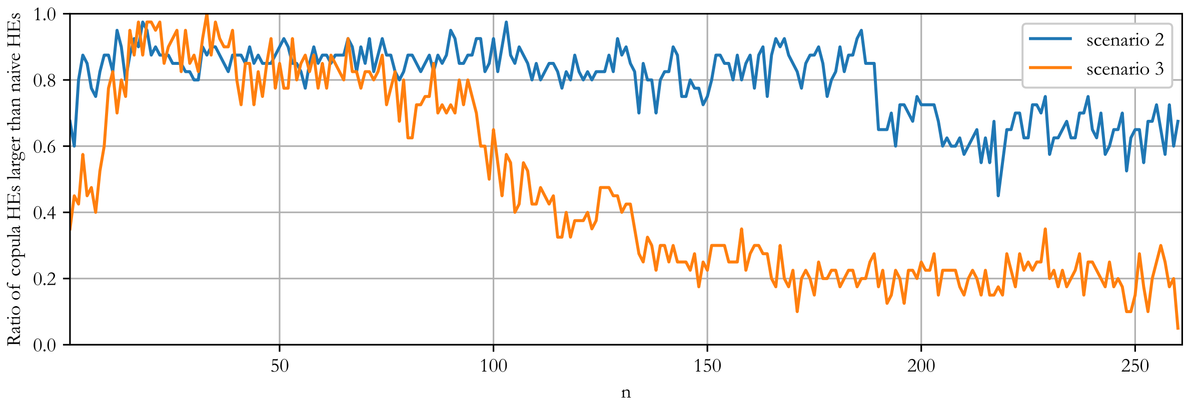

Figure 7: Ratio of positive differences between HOPAC and one-to-one hedging strategy HE to total HEs under HOPAC hedging strategy for scenario two and three (2 scenarios $\times$ 4 HOPACs $\times$ 10 risk measures $= 2 \times 40$ HEs) for lags ranging from 1 to 261 weeks. HEs are computed with the entire loss distribution from from 24 Mar 2000 to 22 Jan 2021 (1087 observations per distribution).

5.5 Hedging Effectiveness

To provide evidence of the efficacy of HOPACs versus one-to-one hedging I compute hedging effectiveness in an out-of-sample study. Table 9 shows hedging effectiveness (HE) for different risk metrics, scenarios and hedging strategies using hedging ratios estimated 20 weeks in advance. Hedging effectiveness is computed by using risk measures on the entire weekly out-of-sample loss distribution from Jul 28 2000 to Jan 22 2021 (5 hedging strategies $\times$ 3 scenarios $\times$ 1069 observations = 15 distributions of 1069 observations). HE is higher relative to one-to-one hedging under the Ali-Mikhai-Haq and Clayton generated HOPACs model for each risk metric when costs are included in trading (scenario 2 and 3). Furthermore, HE is not always greater than one-to-one hedging under the Joe and Frank generated HOPACs when costs are included in trading, but excluded in estimation (scenario 2). Additionally, Joe and Frank generated HOPACs always perform better than one-to-one hedging when costs are included in trading and estimation (scenario 3). Finally, when costs are excluded from trading, some HOPAC models perform worse than one-to-one hedging, which is the most unrealistic case (scenario 1). It seems plausible that, HE performance under different generators is similar because tail dependence are closely related (Table 3). Unsurprisingly, HE is higher for both one-to-one hedging and hedging under HOPAC models when costs are excluded in trading (scenario 1 versus scenario 2 and 3).

Using a sign test (Table 8), I reject the null hypothesis at 2% significance that HOPAC HEs under Ali-Mikai-Haq, Clayton, Frank and Joe generation are equally likely to be higher than one-to-one HE for the VaR risk objectives when costs are excluded or included in estimation, while included in the out-of-sample study. I cannot formally test significance of the null hypothesis for ES because the differences are assumed to be independent, which is not the case for difference ES confidence levels, i.e. ES at 99% is nested in the ES at 98%. I obtain the results by first computing the sign of $HE_i - HE_N$ for $i \in \{A, C, F, J\}$. Then, I count the number of positive signs in scenario 2 and 3 for VaR, and compute the p-value, which is given by $\Pr(X \geq \text{No. positive signs})$ under a binomial distribution with parameter $p = 0.5$ and $n = 10$. The $p-$value is equal to 0.011 under Ali-Mikai-Haq, Frank and Joe generation, and 0.001 under Clayton generation for VaR. While I cannot formally test the ES out-performance, these findings show that modelling prices with HOPACs is the more effective choice for downside risk management relative to one-to-one hedging.

Table 8: P-values of sign test with null hypothesis that HOPAC HEs under Ali-Mikai-Haq, Clayton, Frank and Joe generation are equally likely to be higher than one-to-one HE for the VaR risk objectives when costs are excluded or included in estimation, while included in the out-of-sample study. Results are obtained by counting the number of positive signs in $HE_i - HE_N$ for generators $i \in \{A, C, F, J\}$. P-values are computed by $\Pr(X \geq \text{No. positive signs})$ under a binomial distribution with parameter $p = 0.5$ and $n = 10$, where * shows rejection of the null at 2% significance.

Ali-Mikai-Haq	Clayton	Frank	Joe
0.011*	0.001*	0.011*	0.011*

Table 9: Hedging Effectiveness (HE) in percentage, for generators $i \in \{\text{A, C, F, J}\}$ and one-to-one heding (N). Values are computed for VaR and ES risk measures for significance .9, .93, .95, .98 and .99 and three difference scenarios (see Table 5). Risk measures are computed on the entire weekly out-of-sample loss distribution from Jul 28 2000 to Jan 22 2021 (5 hedging strategies × 3 scenarios × 1069 observations = 15 distributions of 1069 observations). VaR and ES refer to value at risk and expected shortfall, respectively. Furthermore, generators are Ali-Mikai-Haq (A), Clauton (C), Frank (F) and Joe (J).

Risk Measure		HOPAC HE with $n = 20$														
		Scenario 1					Scenario 2					Scenario 3				
Type	$1-\alpha$	HE_N	HE_A	HE_C	HE_F	HE_J	HE_N	HE_A	HE_C	HE_F	HE_J	HE_N	HE_A	HE_C	HE_F	HE_J
VaR	90%	**42.1**	41.7	40.8	39.8	40.7	22.1	22.2	22.7	**23.0**	22.5	22.1	23.9	24.4	22.9	**25.9**
	93%	40.5	41.1	**42.3**	41.1	38.1	23.4	24.4	**24.8**	22.7	21.7	23.4	25.4	**26.3**	25.9	24.9
	95%	36.2	**39.7**	39.5	39.1	39.1	22.0	23.5	**25.5**	24.2	22.9	22.0	24.6	**25.5**	24.4	23.1
	98%	28.9	31.9	29.6	**32.2**	31.7	19.6	**22.3**	19.7	22.2	20.5	19.6	16.8	**21.6**	20.0	20.4
	99%	37.4	38.5	40.5	**43.2**	38.3	29.1	33.5	**34.0**	31.8	32.1	29.1	33.8	**34.7**	32.0	32.1
ES	90%	36.0	36.3	**36.5**	36.4	35.9	23.3	25.0	**25.3**	25.1	24.8	23.3	**24.1**	**24.1**	**24.1**	24.0
	93%	34.7	35.6	**35.7**	35.3	35.0	23.5	25.4	**25.5**	25.1	25.1	23.5	24.2	24.1	**24.3**	24.1
	95%	34.0	**35.0**	34.8	34.7	34.6	24.3	**25.8**	**25.8**	25.5	25.7	24.3	**24.7**	24.6	24.6	**24.7**
	98%	33.3	**34.8**	34.6	34.6	34.0	25.6	**28.2**	27.9	27.7	27.4	25.6	**26.8**	26.2	26.0	26.3
	99%	31.3	32.0	32.3	32.3	**32.7**	24.6	26.4	26.5	26.5	**27.1**	24.6	25.7	25.5	24.8	**25.8**

Table 10: Gross margin difference with one-to-one hedging ($\Delta \mathrm{M}_i$) in percentage, for generators $i \in \{\mathrm{A},\ \mathrm{C},\ \mathrm{F},\ \mathrm{J}\}$. Values are computed for VaR and ES risk measures for significance .9, .93, .95, .98 and .99 and three difference scenarios (see Table 5). on the entire weekly out-of-sample loss distribution from Jul 28 2000 to Jan 22 2021 (5 hedging strategies × 3 scenarios × 1069 observations = 15 distributions of 1069 observations). VaR and ES refer to value at risk and expected shortfall, respectively. Furthermore, generators are Ali-Mikai-Haq (A), Clauton (C), Frank (F) and Joe (J).

Risk Measure		HOPAC HE with $n = 20$							
		Scenario 2				Scenario 3			
Type	$1-\alpha$	$\Delta\mathrm{M_A}$	$\Delta\mathrm{M_C}$	$\Delta\mathrm{M_F}$	$\Delta\mathrm{M_J}$	$\Delta\mathrm{M_A}$	$\Delta\mathrm{M_C}$	$\Delta\mathrm{M_F}$	$\Delta\mathrm{M_J}$
VaR	90%	8.5	10.6	12.6	7.4	45.0	43.0	**46.8**	41.8
	93%	9.5	7.6	9.4	8.1	37.3	35.8	**37.6**	31.1
	95%	3.9	4.6	8.3	1.6	29.1	26.2	**30.1**	24.2
	98%	5.5	8.9	6.8	4.1	17.1	**19.5**	15.2	13.8
	99%	2.2	3.6	3.3	5.3	11.0	10.7	**13.9**	12.1
ES	90%	12.9	12.6	12.7	13.2	36.6	**38.0**	36.5	35.8
	93%	12.8	12.4	12.2	13.1	33.7	**35.9**	33.0	33.2
	95%	12.5	13.3	11.6	13.2	32.5	**34.6**	30.5	31.6
	98%	13.1	14.0	13.1	14.3	30.0	**32.1**	27.0	29.6
	99%	12.4	12.6	13.2	15.7	26.9	**28.9**	25.0	28.3

5.6 Profitability

One of the main responsibilities of managers is to ensure the profitability of their corporation. As such, in this section I provide insights on the effect that including costs in estimation may have on the profitability of refineries. Table 10 shows the difference in gross margin, ΔM_i for $i \in \{A, C, F, J\}$ of one-to-one hedging versus HOPAC hedging for different risk metrics, scenarios and hedging strategies using hedging ratios estimated 20 weeks in advance. The highest gross margin is obtained when costs are included in estimation (scenario 3). The difference between one-to-one and HOPAC hedging is quite substantial for a low margin industry. It seems reasonable that higher margins are caused by the lower-than-one estimated hedging ratios (Table 7). When costs are excluded from estimation, but included in trading (scenario 2), profitability under HOPAC models is still higher than one-to-one hedging, albeit not as large a difference than in scenario 3.

Using a sign test (Table 11), I reject the null hypothesis at 1% significance that HOPAC gross margin difference with one-to-one hedging under Ali-Mikai-Haq, Clayton, Frank and Joe generated HOPACs are positive for the VaR risk objectives when costs are excluded or included in estimation, while included in the out-of-sample study. Again, I cannot formally test significance of the null hypothesis for ES because the differences are assumed to be independent, which is not the case for difference ES confidence levels. I obtain the results by counting the number of positive signs of gross margin differences in scenario 2 and 3 for VaR, and compute the p-value, which is given by $\Pr(X \geq \text{No. positive signs})$ under a binomial distribution with parameter $p = 0.5$ and $n = 10$. The $p-$value is equal to 0.001 for all generators. While I cannot formally test the ES out-performance, these finding show that modelling prices with HOPACs is a more profitable choice for downside risk management relative to one-to-one hedging.

Table 11: P-values of sign test with null hypothesis that HOPAC gross margin difference with one-to-one heding under Ali-Mikai-Haq, Clayton, Frank and Joe generated HOPACs are positive for the VaR risk objectives when costs are excluded or included in estimation, while included in the out-of-sample study. Results are obtained by counting the number of positive signs of gross margin differences in scenario 2 and 3 for VaR, and compute the p-value, which is given by $\Pr(X \geq \text{No. positive signs})$ under a binomial distribution with parameter $p = 0.5$ and $n = 10$, where * shows rejection of the null at 1% significance.

Ali-Mikai-Haq	Clayton	Frank	Joe
0.001*	0.001*	0.001*	0.001*

5.7 Transaction and Margin Costs

Transaction and margin costs are of concern for managers that wish to optimise profitability. Figure 8 shows initial margin, interest, commission and bid-ask spread costs for 99% ES downside risk under (a) one-to-one and (b) Clayton generated HOPAC hedging. Initial margin costs are substantially higher out-of-sample that other costs for ES with a confidence level of 99% in scenario 3 from Jul 28 2000 to 22 Jan 2021. Furthermore, commission and bid-ask spread costs are negligible relative initial margin and interest costs. Additionally, interest costs can be positive and negative, while all other costs are positive only. Furthermore, interest costs become negligible when interest rates are low. Moreover, initial margin costs appear to be more volatile albeit lower for the Clayton generated HOPAC strategy than the one-to-one strategy.

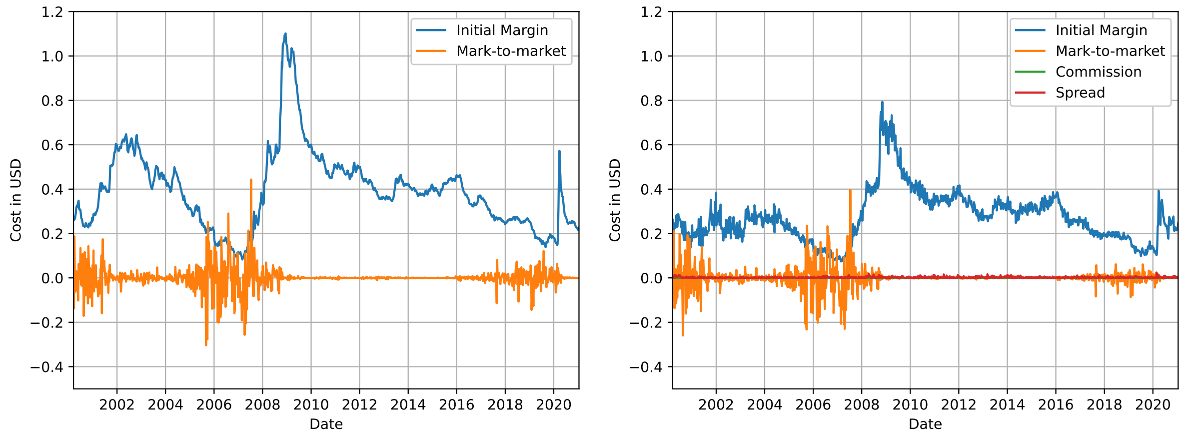

(a) (b)

Figure 8: (a) Initial margin and interest costs per barrel for the one-to-one hedging strategy and ES with a confidence level of 99% risk objective in scenario 3 from 17 Mar 2000 to 21 Mar 2021, (b) Initial margin, interest costs, commission and bid-ask spread per barrel for the Clayton generated HOPAC hedging strategy and ES with a confidence level of 99% risk objective in scenario 3 from Jul 28 2000 to 22 Jan 2021

Initial margin costs appear to increase substantially post Dot-com bubble, Great Recession and COVID-19 pandemic in 2000, 2008 and 2020, respectively. These periods are particularly relevant because they generally coincide with large swings in petroleum prices, when demand undercuts the current supply. This increase in initial costs can be explained by the increase in spread between borrowing costs for oil refineries and subsequent lowering of interest rates by central banks to stimulate the economy. It should be noted that, future recessions may be very different for oil refineries, as central banks have changed policies in the past, and credit rating of oil refineries may worsen of improve. This may increase or decrease the spike of initial margin costs in and after future recessions.

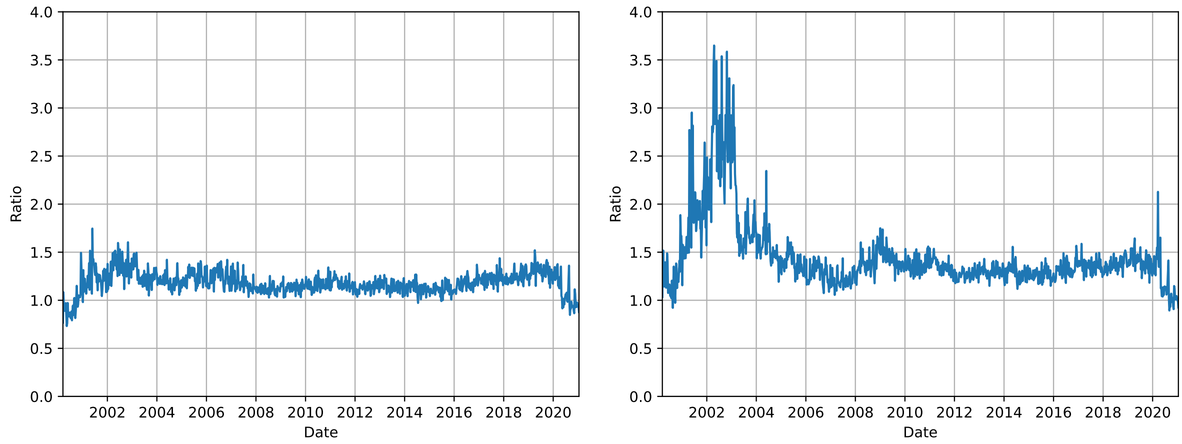

(a) (b)

Figure 9: (a) Initial margin ratio for the one-to-one hedging strategy and ES with a confidence level of 99% risk objective in scenario 2 from Jul 28 2000 to 22 Jan 2021, (b) Initial margin ratio for the one-to-one hedging strategy and ES with a confidence level of 99% risk objective in scenario 3 fromJul 28 2000 to 22 Jan 2021. Initial margin ratio is defined as initial margin under one-to-one strategy devided by intitial margin under Clayton generate HOPAC strategy.

Figure 9 shows initial margin ratio of one-to-one and Clayton generated HOPAC hedging for 99% ES downside risk and scenario 2 and 3. This confirms that initial margin costs are lower for the HOPAC strategy relative to the one-to-one strategy for both scenario 2 and 3 most of the time. Additionally, the difference increases when costs are included in estimation in scenario 3. Thus, including costs in estimation effectively decreases costs out-of-sample. This may explains the difference in gross margin between one-to-one and Clayton generated HOPAC strategy in Table 10.

6 Discussion & Conclusion

Managers of refineries are confronted with risk management decisions due to their exposure to downside risk in a multi-product petroleum market. Refineries can hedge downside risk exposure using crude oil, heating oil and gasoline futures contracts. This study proposes a multi-product hedging strategy to minimise downside risk of oil refineries, measure by value at risk and expected shortfall.

The HOPAC hedging strategy presented in this study outperforms the 'hard-to-beat' one-to-one downside risk hedging of oil refineries. It seems plausible that the structured, skewed and asymmetrical HOPACs are well suited for modelling petroleum price changes. In addition, I show that including transaction and margin costs in estimation successfully increases gross margins, while outperforming one-to-one hedging still. Moreover, initial margin costs are the most important consideration for managers that wish to optimise profitability while hedging.

In an out-of-sample setting, I find that modelling price changes with Ali-Mikhai-Haq, Clayton, Frank and Joe generated HOPACs outperforms one-to-one hedging in a VaR and ES downside risk setting. This result is obtained by including transaction and margin costs directly into the estimation and trading. Additionally, I find that the optimal forecast lag is 20 weeks. Furthermore, gross margins are higher relative to one-to-one hedging and increases with tens of basis points when transaction and margin costs are included in estimation. Finally, initial margin costs are most important for managers to consider, especially in troubling economic times such as during the Great Recession and novel coronavirus pandemic. This is caused by an increase in borrowing costs, as investors require a higher return when risks increase, and decrease in risk free rate, as central banks try to support the economy.

The fact that modelling commodity price changes with HOPACs outperforms one-to-one hedging can be explained by (i) the stability of the structure of spot and future prices, (ii) asymmetrical marginals due to supply and demand characteristics of the underlying commodities and (iii) non-normality in price changes that are captured by the model. Additionally, HOPACs are relatively parsimonious leading to more robust hedging ratios than other proposed models in literature, e.g. Sukcharoen and Leatham (2017) and Lui et al. (2017), while still outperforming one-to-one hedging. Higher profitability may be explained by lower hedging ratios, that lead to lower initial margin costs, especially when costs are included in estimation. I conclude that managers that are interested in downside risk hedging of oil refineries should consider modelling price changes with HOPACs with inclusion of transaction and margin costs in the estimation process.

However, this result was obtained on weekly data form 17 Mar 1995 to 12 Mar 2021, and may change in future periods. Moreover, including transaction and margin costs in estimation improve profitability out-of-sample, but increase the volatility of hedging ratios. Furthermore, seasonality in gasoline prices may drag on the model estimation. I suspect, that filtering for this specific seasonality may improve the fit of the model.

References

Alexander, C., Prokopczuk, M., & Sumawong, A. (2013). The (de)merits of minimum-variance hedging: Application to the crack spread. *Energy Economics*, *36*, 698–707.

Chan, W., & Maheu, J. (2002). Conditional jump dynamics in stock market returns. *Journal of Business & Economic Statistics*, *20*, 377–389.

Dunis, C., Laws, J., & Evans, B. (2008). Trading futures spread portfolios: Applications of higher order recurrent networks. *The European Journal of Finance*, *14*, 503–521.

Energy Information Administration. (2002). *Derivatives and risk management in the petroleum, natural gas, and electricity industries.* U.S. Department of Energy.

Galai, D. (1979). A proposal for indexes for traded call options. *The Journal of Finance*, *34*, 1157–1172.

Górecki, J., Hofert, M., & Holeňa, M. (2017). On structure, family and parameter estimation of hierarchical Archimedean copulas. *Journal of Statistical Computation and Simulation*, *87*(17), 3261–3324.

Górecki, J., Hofert, M., & Okhrin, O. (2021). Outer power transformations of hierarchical Archimedean copulas: Construction, sampling and estimation. *Computational Statistics and Data Analysis*, *155*, 107109.

Haigh, M., & Holt, M. (2002). Crack spread hedging: Accounting for time-varying volatility spillovers in the energy futures market. *Journal of Applied Econometrics*, *17*(3), 269–289.

Hofert, M. (2010). *Sampling nested archimedean copulas with applications to CDO pricing.* Universitat Ulm.

Hofert, M. (2011). Efficiently sampling nested archimedean copulas. *Computational Statistics and Data Analysis*, *55*, 57–70.

Ji, Q., & Fan, Y. (2011). A dynamic hedging approach for refineries in multiproduct oil markets. *Energy*, *36*, 881–887.

Joe, H. (1997). *Multivariate models and dependence concepts.* Chapman & Hall.

Lai, J. (2012). An empirical study of the impact of skewness and kurtosis on hedging decisions. *Quantitative Finance*, *12*(12), 1827–1837.

Lien, D., & Tse, Y. (1998). Hedging time-varying downside risk. *The Journal of Futures Markets*, *18*(6), 705–722.

Lui, P., Vedenov, D., & Power, G. (2017). Is hedging the crack spread no longer all it's cracked up to be? *Energy Economics*, *63*, 31–40.

Maheu, J., & McCurdy, T. (2004). News arrival, jump dynamics and volatility components for individual stock returns. *Journal of Finance*, *59*, 755–793.

McNeil, A. (2008). Sampling nested Archimedean copulas. *Journal of Statistical Computation and Simulation*, *78*(6), 567–581.

McNeil, A., Frey, R., & Embrechts, P. (2015). *Quantitative risk management: Concepts, techniques and tools.* Princeton University Press.

Nelder, J., & Mead, R. (1965). A simplex method for function minimization. *The Computer Journal*, *7*(4), 308–313.

Nelsen, R. (2006). *An introduction to copulas.* Springer-Verlag.

Ostap, O., Okhrin, Y., & Wolfgang, S. (2013). On the structure and estimation of hierarchical archimedean copulas. *Journal of Econometrics*, *173*, 189–204.

Peng, J., Li, Z., & Drakeford, B. (2020). Dynamic characteristics of crude oil price fluctuation - from the perspective of crude oil price influence mechanism. *Energies*, *13*, 4465.

Salisu, A., & Fasanya, I. (2013). Modelling oil price volatility with structural breaks. *Energy Policy*, *52*, 554–562.

Sklar, A. (1957). Fonctions de répartition à n dimensions et leurs marges. *Publications de l'Institut Statistique de l'Université de Paris 8*, 229–231.

Sukcharoen, K., Choi, H., & Leatham, D. (2015). Optimal gasoline hedging strategies using futures contracts and exchange-traded funds. *Applied Economics*, *47*(32), 3482–3498.

Sukcharoen, K., & Leatham, D. (2017). Hedging downside risk of oil refineries: A vine copula approach. *Energy Economics*, *66*, 493–507.

The Energy Data Modeling Center. (2006). *Supply and demand analysis on petroleum products and crude oils for asia and the world.* The Institute of Energy Economy, Japan.